

# ESTIMATE OF FREE ELECTRON LASER GAIN LENGTH IN THE PRESENCE OF ELECTRON BEAM COLLECTIVE EFFECTS\*

S. Di Mitri<sup>#</sup>

Elettra Sincrotrone Trieste, 34149 Basovizza, Trieste, Italy

S. Spampinati

Department of Physics, University of Liverpool, Liverpool L69 7ZX, United Kingdom

Cockcroft Institute, Sci-Tech Daresbury, Warrington WA4 4AD, United Kingdom

## Abstract

A novel definition for the three-dimensional free electron laser gain length is proposed [1], which takes into account the increase of electron beam projected emittance as due, for example, to geometric transverse wakefield and coherent synchrotron radiation developing in linear accelerators. The analysis shows that the gain length is affected by an increase of the electron beam projected emittance, even though the slice (local) emittance is preserved, and found to be in agreement with Genesis code simulation results. It is then shown that the minimum gain length and the maximum of output power may notably differ from the ones derived when collective effects are neglected. The proposed model turns out to be handy for a parametric study of electron beam six-dimensional brightness and FEL performance as function, e.g., of bunch length compression factor, accelerator alignment tolerances and optics design.

## WORK PLAN

Following our work in [1], which relies in turn on the formalism developed in [2,3,4]:

- We analytically evaluate the electron beam 6-D energy-normalized brightness,  $B_{n,6D}$ , in the presence of short-range geometric transverse wakefield (GTW) in accelerating structures and coherent synchrotron radiation (CSR) emitted in magnetic compressors. We extend our previous study [5] to include the analytical estimate of the final slice energy spread when microbunching instability (MBI) is suppressed with a laser heater [6]. This estimate makes use of the analytical model for the MBI given in [7,8].

- We show that the physical picture proposed in [4] for the beam motion in an undulator also applies to angular perturbations caused by GTW and CSR in the accelerator. Consequently, we establish an explicit connection between the FEL performance, so far only predicted on the basis of the electron bunch's slice parameters, and a more complete set of sources of  $B_{n,6D}$  degradation that is including projected beam parameters.

- An analytical formula is given for estimating the self-amplified spontaneous emission (SASE) FEL [9,10] 3-D power gain length's [11] increase due to collective effects, the power saturation length and the peak power at saturation. We extend the discussion beyond SASE to the

case of externally seeded FELs.

## THEORETICAL MODEL

GTW and CSR offset individual “macro-slices” both in configuration and velocity spaces. The macro-slices are modelled to be as long as several cooperation lengths, since GTW and CSR-induced transverse kicks are typically correlated with  $z$ , the longitudinal coordinate internal to the bunch, on the length scale of few to hundreds microns. Neglecting for the moment any slice emittance growth from the injector to the undulator, the projected emittance growth is entirely due to mismatch of the bunch macro-slices in the transverse phase space. We take this growth into account through the mechanism described by Tanaka *et al.* [4]. In that work, the authors identify two distinct processes that increase  $L_{g,1D}$ . One is a lack of overlapping between the spontaneous undulator radiation, whose wavefront follows the electrons' local direction of motion, and the FEL radiation, whose wavefront is preserved when the electrons are transversally kicked by lattice errors. The other process is electrons' bunching smearing due to longitudinal dispersion of electrons transversally kicked by lattice errors.

We recognize that the electrons' angular divergence has two contributions: one is incoherent and due to the finite beam emittance as depicted in Xie's [11] and Saldin's [12] models; the other is coherent, being the tilt of the macro-slice centroids with respect to the reference trajectory. The coherent divergence adds to (and in some cases, surpasses) the incoherent one and may amplify the effect of bunching smearing. In order to take into account the coherent motion of electrons, we apply the physical picture depicted in [4] to individual macro-slices. Each macro-slice is transversally kicked by collective effects in the linac and thus moves along the undulator on a different trajectory than other macro-slices, as shown in Fig. 1.

We call  $\sqrt{\langle \theta_{coll}^2 \rangle}$  the rms angular divergence of the macro-slice centroids at the undulator. Being a quantity averaged over the bunch duration,  $\sqrt{\langle \theta_{coll}^2 \rangle}$  is an indicator of the mismatch of the macro-slices in the transverse phase space, projected onto the  $z$ -coordinate. We assume that the charge transverse distribution at the undulator is matched to some design Twiss parameters, and that a smooth optics is implemented along the

\*Work supported by the FERMI project of Elettra Sincrotrone Trieste.

<sup>#</sup>simone.dimitri@elettra.eu

undulator line:  $\beta_u$  is the average betatron function and its variation is small along the undulator. Thus, the determinant of the so-called “sigma matrix” computed at the undulator provides the beam projected emittance as a function of  $\sqrt{\langle \theta_{coll}^2 \rangle}$  and  $\beta_u$  [1]:

$$\varepsilon_{n,f} \approx \varepsilon_{n,0} \sqrt{1 + \frac{\gamma \beta_u \langle \theta_{coll}^2 \rangle}{\varepsilon_{n,0}}}, \quad (1)$$

with  $\varepsilon_{n,0}$ ,  $\varepsilon_{n,f}$  being the rms initial (unperturbed) normalized and the final normalized emittance in the plane of interest, respectively, and  $\gamma$  the relativistic Lorentz factor at the undulator. Finally, we revise Tanaka’s formula for the gain length [4] and make the following ansatz to estimate the 3-D gain length in the presence of collective effects [1]:

$$L_{g, coll} \approx \frac{L_{g, 3D}}{1 - \pi \langle \theta_{coll}^2 \rangle / \theta_{th}^2}, \quad (2)$$

$L_{g, 3D}$  is the 3-D power gain length in the sense of Xie [11];  $\theta_{th} = \sqrt{\lambda / L_{g, 3D}}$  and  $\lambda$  the FEL wavelength. The electron beam slice transverse emittance and the slice energy spread at the undulator are taken into account in  $L_{g, 3D}$ ; the information on the degradation of the projected emittance is brought about by  $\langle \theta_{coll}^2 \rangle$ . The range of application of Eq.2 is  $\langle \theta_{coll}^2 \rangle < \theta_{th}^2 / \pi$ ; larger values of are assumed to inhibit the FEL process.

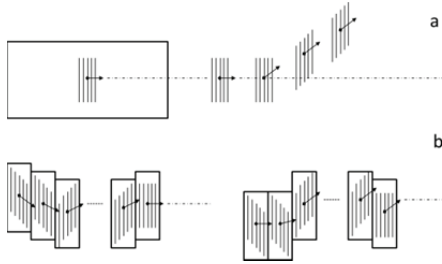


Figure 1: Effect of a transverse kick on electrons in an undulator. (a) All electrons in the bunch follow the same direction of motion as a whole. (b) Different macro-slices in the same bunch follow different directions of motion along the undulator by virtue of their initial different launching conditions. In the sketch, solid lines define the bunch (a) or a macro-slice (b); arrows indicate the electrons’ direction of motion; vertical bars identify the FEL microbunch wavefront orientation. Copyright of American Physical Society [1].

## DEPENDENCE ON THE BEAM OPTICS

Equation 2 aims to generalize Xie’s formalism, so that  $L_{g, coll}$  reduces to  $L_{g, 3D}$  either for null collective effects  $\langle \theta_{coll}^2 \rangle = 0$  or large  $\beta_u$ , for any *pre-set* emittance growth (see Eq.1). The dependence on  $\beta_u$  is explained as follows.

We assume an electron beam whose normalized emittance grows along the linac according to  $\Delta \varepsilon_n = \varepsilon_{n,f} - \varepsilon_{n,0}$ . If such a growth only concerns the slice emittance, the gain length will be  $L_{g, 3D}$  according to [11]. If, instead, the emittance growth is only the projected one, and the slice emittance is preserved at the injector level, the gain length will be  $L_{g, coll}$  in Eq.2. We point out that, in this modeling, the *projected* growth  $\Delta \varepsilon_n$  is uniquely determined by the initial beam parameters and the linac setting and, as already said, it is due to the bunch slices’ misalignment in the transverse phase space. Then, if  $\beta_u$  is large, as in a weak focusing undulator lattice, the macro-slices will tend to overlap in angular divergence, that is  $\langle \theta_{coll}^2 \rangle \rightarrow 0$ , as shown in Fig. 2-d. In this case we expect  $L_{g, coll}$  to approach  $L_{g, 3D}$ . On the contrary, a small  $\beta_u$  as due, *e.g.*, by strong focusing, will force the macro-slice centroids to very different angular divergences. In this case  $\langle \theta_{coll}^2 \rangle \neq 0$  as shown in Fig. 2-c, and we expect  $L_{g, coll}$  to diverge from  $L_{g, 3D}$ .

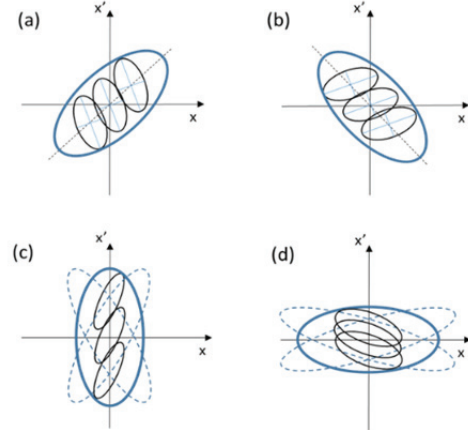


Figure 2: Mechanism of emittance growth in the transverse phase space, due to kicks by collective effects (cartoon). (a) Two macro-slices are displaced along the direction of the kick (dashed line) with respect to an unperturbed macro-slice (inner centered ellipse). The projected emittance has grown (outer ellipse). (b) Same as in (a), after  $\pi/2$  betatron phase advance. The area of the outer ellipse remains constant after the kick. (c) The beam is matched at the entrance of the undulator to some design Twiss parameters. The optics is smooth in a way that Twiss parameters  $\beta$  and  $\alpha$  vary little along the undulator (dashed outer ellipses). Since  $\beta_u$  is small, the macro-slices are largely dispersed in angular divergence that is (solid line ellipse). (d) Same as in (c), but with  $\beta_u$  large. The macro-slices largely overlap in angular divergence that is (solid line ellipse). Copyright of American Physical Society [1].

The parameters listed in Table.1 are considered for a quantitative comparison of  $L_{g, coll}$  and the M.Xie-defined  $L_{g, 3D}$  as function of  $\beta_u$ , in Fig. 3. The FEL wavelength and the emittance growth were chosen in order to ensure  $\langle \theta_{coll}^2 \rangle < \theta_{th}^2 / \pi$  over the entire range of  $\beta_u$ .  $L_{g, 3D}$  was

computed for beam slice normalized emittances of  $0.5 \mu\text{m}$  (green dashed-dotted line) and  $2.3 \mu\text{m}$  (red dashed line); in these cases the projected emittances coincide with the sliced values since all slices are well aligned in the phase space.  $L_{g,\text{coll}}$ , instead, was computed for a beam slice normalized emittance of  $0.5 \mu\text{m}$  and  $2.3 \mu\text{m}$  normalized projected emittance (blue solid line). The latter is determined by the misalignment of the bunch slices in the phase space. The analytical predictions are in agreement with the simulation results obtained with the Genesis code [13], over the entire range of  $\beta_u$  considered (symbols), thus demonstrating the validity of the proposed gain length model and its consistency with the existing 3-D theory.

Most of VUV and x-ray FELs, existing and planned, tend to have  $\beta_u$  small in order to maximize the transverse overlap of electrons and photons in the undulator. Figure 3 suggests that a beam focusing less tight than foreseen for an ideal beam might be more suitable in the presence of a highly diluted projected emittance.

Table 1. Parameters for the SASE FEL used to compare  $L_{g,\text{coll}}$  (Eq.2) and  $L_{g,3D}$  [11], as function of  $\beta_u$

Parameter	Value	Unit
Energy	1.8	GeV
Peak Current	3.0	kA
Norm. Transv. Emittance at the Injector, rms	0.5	$\mu\text{m}$ rad
Norm. Transv. Emittance at the Undulator, rms	2.3	$\mu\text{m}$ rad
Undulator Parameter (Planar Undulator), K	$\sqrt{2}$	
Undulator Period	20	mm
FEL Parameter, 1-D (for $\beta_u = 10\text{m}$ )	0.1	%

The physics depicted so far applies in principle both to SASE and to externally seeded FELs because, independently from the FEL start-up signal, they both rely on the amplification of undulator radiation through the formation of bunching at the resonance wavelength. In practice, however, in a SASE FEL the entire bunch participates to lasing, while for externally seeded FELs only the seeded portion of the electron bunch is relevant to lasing. In other words, the present analysis applies only to the lasing (seeded) portion of the electron bunch.

## BRIGHTNESS AND FEL PERFORMANCE

The *electron* 6-D normalized electron beam brightness,  $B_{n,6D}$ , is defined as the total bunch charge over the product of the horizontal, vertical and longitudinal rms normalized *projected* emittance. The normalized longitudinal emittance is the product of bunch length and absolute energy spread. All three emittances are invariant under acceleration and linear bunch length compression, but are degraded by collective effects, i.e. CSR and GTW. These effects are modelled as angular kicks to the particles' coordinate. The final normalized emittance subjected to CSR in  $n$  consecutive compression stages and to GTW in  $m$  linac sections, is provided by the

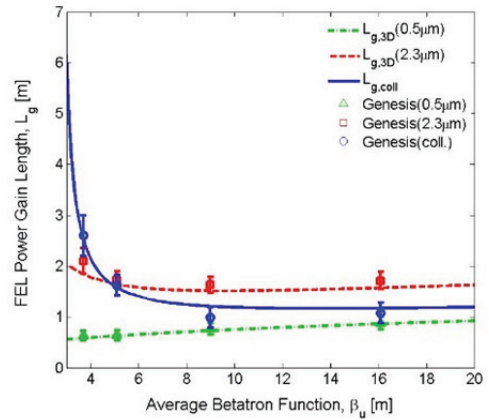


Figure 3: Gain length as function of the average betatron function in the undulator, analytical (lines) and from Genesis simulation (symbols), with parameters from Tab.1. The gain length from simulations fits the FEL power growth along the undulator. Error bars show the maximum variation of the fit value over several runs. For each run used to fit  $L_{g,\text{coll}}$  (blue circles), several random distributions of the bunch's macro-slices in the transverse phase space were generated. In this case, each distribution (in each transverse plane) corresponds to a normalized projected emittance of  $2.3 \mu\text{m}$ , while the slice emittance is  $0.5 \mu\text{m}$  for all slices. The projected beam size is forced to fit the average betatron function selected for that run. Copyright of American Physical Society [1].

determinant of the “sigma matrix” computed at the linac end in the presence of those kicks. Since the emittance is also defined in Eq.1, we can compute  $\langle \theta_{\text{coll}}^2 \rangle$  as a function of the perturbations once  $\beta_u$  and  $\varepsilon_{n,f}$  are known.

We consider a single-pass linac driving SASE FEL in the ultra-violet wavelength range (see [1] for list of parameters). We investigated two options: one-stage compression at low energy and two-stage compression with fixed total compression factor  $C = C1 \times C2$ . We then looked at  $B_{n,6D}$  versus  $C1$  to identify the compression scheme that maximizes the beam brightness for a given final peak current (1 kA), as shown in Fig. 4. That compression scheme was then used to compare in Fig. 5 the FEL 3-D output performance gain length in the presence of collective effects to those predicted by M.Xie. Finally, we selected the compression factor that minimizes  $L_{g,\text{coll}}$  and, in Fig. 6, studied its sensitivity, as well as that of  $B_{n,6D}$ , to the linac-to-beam misalignment and the optics in the compressor.

## CONCLUSIONS

We have extended the existing analytical models for the estimation of the electron beam brightness and of FEL properties – gain length, saturation length and power at saturation of a SASE FEL – by including the collective effects in the driving linac. Two major findings follow from the proposed model:

1) The degradation of the beam transverse projected emittance affects the FEL performance even though the

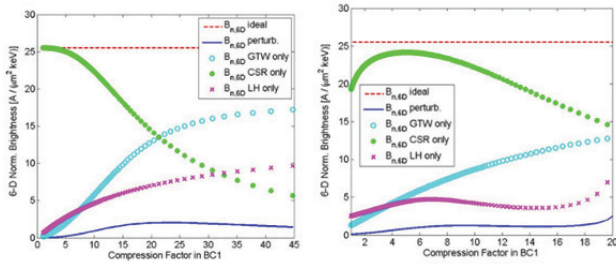


Figure 4: Analytical estimate of final  $B_{n,6D}$  for the one-stage (left) and two-stage compression, as function of the compression factor in BC1. In the two-stage, the total compression factor is fixed to 20. Copyright of American Physical Society [1].

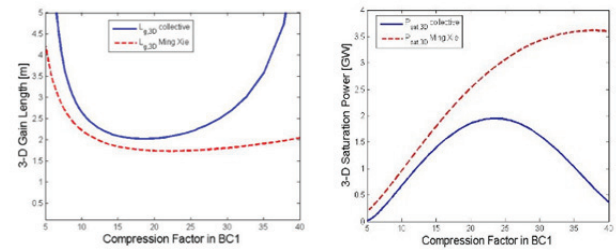


Figure 5: The 3-D gain length (left), and the 3-D SASE saturation power are evaluated in the M. Xie sense and in presence of collective effects. Copyright of American Physical Society [1].

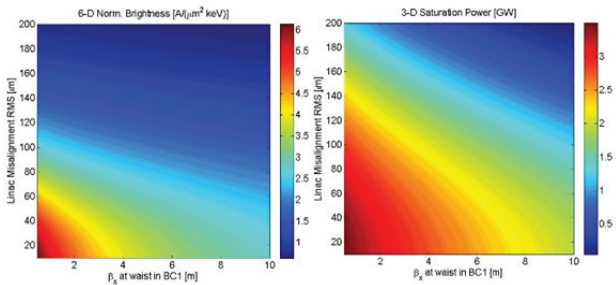


Figure 6: Contour plot of  $B_{n,6D}$  (left) and  $P_{sat,coll}$  as function of the rms linac-to-beam misalignment and of the minimum betatron function in BC1. A 500 pC bunch charge, compressed in one-stage by a factor 18. The final peak current is 0.9 kA. Copyright of American Physical Society [1].

slice emittance is preserved. Our analytical finding for the 3-D gain length in the presence of collective effects, *i.e.* Eq.2, is in agreement with Genesis simulation results within 5%–15% of the gain length, over the wide range of  $\beta_u$  considered (see Fig.3). The residual analysis *vs.* simulation discrepancy may originate from the lack of several approximations in the Genesis runs, which are instead part of our theory: the asymmetry of horizontal and vertical betatron function (at large  $\beta_u$ ) whereas our model assumes perfect symmetry; the effect of multiple angular kicks on the bunch’s macro-slices by offset

quadrupole magnets, which are neglected in our model; the power gain computed from time-dependent simulations instead of the steady-state approximation (single longitudinal FEL mode), which is part of Tanaka’s model.

2) The enlargement of the FEL power gain length due to a dilution of the projected emittance can be counteracted by a relatively large average betatron function in the undulator line. The optimum value of the average betatron function (*i.e.*, corresponding to the minimum gain length) turns out to be closer to the value dictated by the projected emittance with respect to that associated to the slice emittance.

Our model was then compared with that by Xie [11], with the following quantitative findings:

- i) A deterioration of the FEL performance with respect to Xie’s model is observed when collective effects are included. For the cases considered here, a discrepancy of ~15% between  $L_{g,3D}$  and  $L_{g,coll}$  is observed around the point of minimum gain length, and a much larger discrepancy at very small and very large values of C1.
- ii) The collective effects halve the “good” range of C1 over which the gain length and the saturation length are little sensitive (*i.e.*, vary less than 10%) to the compression factor.
- iii) The SASE power at saturation in the Xie’s sense is reduced by the collective effects by a factor up to 3 in the C1 range considered.

The proposed analysis does not pretend to replace sophisticated FEL codes. Our analysis may be useful for an initial exploration of the design parameters of a high brightness linac-driven FEL and of the magnetic lattice in the undulator line. As a matter of fact, the analytical model described in this article allowed us to investigate and to optimize, as a practical case study, an accelerator layout by inspecting two compression schemes, and to scan the FEL properties *vs.* the compression strength, the linac-to-beam misalignment, and the betatron function in the magnetic compressor. Our study establishes the predominant influence of GTW on  $B_{n,6D}$  for a high charge beam driven by an S-band linac, and that of CSR for a low charge beam in an X-band FEL driver (not shown). We observed a net dependence of the FEL saturation power on  $B_{n,6D}$ . We also found that the gain length and the saturation length can be made quite insensitive to the linac-to-beam misalignment (*i.e.*, GTW instability) and to the optics in the compressor (*i.e.*, CSR instability) with a proper choice of the compression scheme and strength.

### ACKNOWLEDGEMENTS

The authors are in debt with M. Cornacchia for his encouragement, and with W. Fawley for stimulating discussions about the dependence of FEL performance on the beam optics. We acknowledge A. Zholents for his suggestion to extend our work to the 6-D brightness, and E. Allaria and for his advices on FEL physics. This work was funded by the FERMI project of Elettra Sincrotrone Trieste.

## REFERENCES

- [1] S. Di Mitri and S. Spampinati, Phys. Rev. Special Topics – Accel. Beams **17**, 110702 (2014).
- [2] M. Xie, in Proc. of Part. Accel. Conf. 1995, TPG10, IEEE (1996).
- [3] E. L. Saldin, E. A. Schneidmiller and M. V. Yurkov, in Proc. of the 26th Free Electron laser Conf., MOPOS15, Trieste, Italy (2004).
- [4] T. Tanaka, H. Kitamura and T. Shintake, Nucl. Instrum. Methods Phys. Research A **528** (2004) 172–178.
- [5] S. Di Mitri, Phys. Rev. Special Topics – Accel. Beams **16**, 050701 (2013).
- [6] E. L. Saldin, E. A. Schneidmiller and M. V. Yurkov, Nucl. Instrum. Methods Phys. Res., Sect. A **528** (2004) 355.
- [7] Z. Huang and K.-J. Kim, Phys. Rev. Special Topics – Accel. Beams **5**, 074401 (2002).
- [8] Z. Huang, M. Borland, P. Emma, J. Wu, C. Limborg, G. Stupakov and J. Welch, Phys. Rev. Special Topics – Accel. Beams **7**, 074401 (2004).
- [9] R. Bonifacio, C. Pellegrini and L. Narducci, Opt. Commun. **50** (1984) 373-378.
- [10] A. M. Kondratenko and E.L. Saldin, Part. Accel. **10** (1980) 207–216.
- [11] M. Xie, in Proc. of Part. Accel. Conf. 1995, TPG10, IEEE (1996).
- [12] L. Saldin, E. A. Schneidmiller and M. V. Yurkov, in Proc. of the 26<sup>th</sup> Free Electron laser Conf., MOPOS15, Trieste, Italy (2004).
- [13] S. Reiche et al., in Proc. of the 22<sup>nd</sup> Part. Accel. Conf., TUPMS038, Albuquerque, NM, USA (2007): <http://pbpl.physics.ucla.edu/>